

Optical properties of a hurricane

Alexander A. Kokhanovsky*, W. von Hoyningen-Huene

Institute of Environmental Physics, University of Bremen, D28334 Bremen, Germany

Received 11 November 2002; accepted 21 September 2003

Abstract

This paper is devoted to study of the distribution of the reflection function, spherical albedo, and optical thickness for a hurricane Erin, located in the western Atlantic (39.3°N , 60.4°W) on September 13th, 2001(16:21 UTC). The limitations and possibilities of using SeaWiFS imagery for remote sensing of hurricanes are discussed. In particular, it is found that the mode of the hurricane spherical albedo spatial distribution is equal to 0.86 and the transport optical thickness is in the range 4–10 on average for the central core of a hurricane. A simple analytical method to derive the hurricane optical thickness distribution is proposed.

© 2004 Elsevier B.V. All rights reserved.

Keywords: Hurricane; Optical thickness distribution; SeaWiFS

1. Introduction

By definition, hurricanes contain winds in excess 119 km/h and large areas of heavy rainfall. Therefore, they belong to one of the most dangerous natural hazards. This explains the great interest in the hurricane research especially in recent years (Simpson, 2002). Physical characteristics of hurricanes are usually obtained using radar remote sensing techniques (Heymsfield et al., 2001). The optical imagery serves as an important tool for a timely identification of hurricanes and for tracking their trajectories (especially where radar is not available).

The optical remote sensing techniques (King et al., 1992) also can be used to study physical characteristics of hurricanes like hurricane-top height, the liquid water path, the thermodynamic phase of particles and their approximate size. The enhanced spatial

* Corresponding author.

E-mail address: alexk@iup.physik.uni-bremen.de (A.A. Kokhanovsky).

resolution of optical imagery allows for important complimentary information as compared to microwave techniques.

In particular, the hurricane-top height can be retrieved from the depth and the profile of the oxygen A-line (Yamamoto and Wark, 1961; Fisher et al., 1991; Koelemeijer et al., 2001). It is known that this line is very strong in the cloudless atmosphere. However, the depth of the oxygen A-line decreases for cases such as a hurricane. This is because most of photons are reflected by a hurricane. Therefore, they can not propagate down to the surface and be absorbed by oxygen there.

The thermodynamic phase of particles in a hurricane can be retrieved using different spectral behaviour of ice and water in selected channels (Knap et al., 2002). Also, the angular behaviour of the degree of polarization of reflected light can be used. This differs for ice crystals and spherical water droplets (Goloub et al., 2000). The size of particles can be estimated from water/ice absorbing wavelength λ [e.g., around 2.16 μm where gaseous absorption is negligible (Nakajima et al., 1991)]. Then, knowing the hurricane optical thickness, which is easily determined from a visible channel (e.g., around 400 nm, where reflection from ocean is low), one also can find the liquid water path and the total weight of water stored in a hurricane.

Therefore, studies of optical, geometrical, and microphysical properties of hurricanes can be performed using standard cloud retrieval techniques (Nakajima et al., 1991).

Clearly, some additional difficulties and problems can arise in this case. They are related mostly to the relative importance of 3-D effects (e.g., in a hurricane wall), scattering by nonspherical particles and large values of the geometrical and optical thickness of hurricanes.

This paper is devoted to the discussion of limitations and possibilities related to optical remote sensing techniques as applied to the hurricane optical thickness τ and the liquid water path W determination. This is done using one characteristic example, namely the case of the hurricane Erin.

Erin can be traced back to a tropical wave that emerged from the western Africa on August 30th, 2001. The hurricane took a long journey from the coast of Africa to the northern Leeward Islands and then to Greenland over the western Atlantic before it merged with high-latitude cyclonic flow on September 17th, 2001. Note that this hurricane was the first one for which a comprehensive three-dimensional image of the complete inner core (including the eyewall and the eye) has been created.

We also studied the aerosol optical thickness distribution of the area, which surrounded the hurricane. This information can be used for better understanding of a hurricane's internal structure and aerosol loading of air masses around a hurricane.

Note that the weight (total amount of water stored) in a hurricane can be estimated from the information on the optical thickness spatial distribution. This is due to the well-known relationship between the liquid/ice water path W and the optical thickness τ (Kokhanovsky, 2001):

$$W = A\tau, \quad (1)$$

where $A = 2/(3\rho a_{\text{ef}})$, ρ is the density of water/ice and a_{ef} is the effective size of particles, defined as the ratio of the average volume of particles to their average surface area,

multiplied by 3. This coincides with the ratio of the third to the second moment of the particle size distribution in the case of spherical particles.

Thus, the liquid water path spatial distribution is given by the spatial distribution of the optical thickness in the assumption that the values of a_{ef} and ρ do not vary.

In addition, the total amount of water is

$$M = \int_S W(s) \, ds, \quad (2)$$

where S is the hurricane's total area and ds is the elementary area.

The retrieval procedure is performed using the SeaWiFS local area coverage imagery with the spatial resolution of about 1×1 km, taken on September 13th, 2001 (16:21UTC).

2. The reflection function of a hurricane

The SeaWiFS instrument measures the top-of-atmosphere backscattered light intensity $I(\xi, \eta, \phi)$ in eight channels (412, 443, 490, 510, 555, 670, 765, and 865 nm). Here $\xi = \cos \vartheta_0$ is the cosine of the solar zenith angle ϑ_0 , $\eta = \cos \vartheta$ is the cosine of the observation zenith angle ϑ , and ϕ is the relative azimuth. The solar extraterrestrial irradiance $F_0(\lambda)$ is obtained from the paper by [Neckel and Labs \(1989\)](#) by averaging with account for the SeaWiFS bandwidth. Only data for the wavelength 412 nm are used in this study. This is due to a low spectral variation of a hurricane reflectance, which is due to large size a of particles (as compared to the light wavelength) in a hurricane ([Deirmendjian, 1969](#)).

It is more convenient to deal with the reflection function $R(\xi, \eta, \phi)$ than with the light intensity $I(\xi, \eta, \phi)$. The reflection function is defined as follows

$$R(\xi, \eta, \phi) = \frac{\pi I(\xi, \eta, \phi)}{F_0(\lambda) \xi}. \quad (3)$$

From Eq. (3),

$$I(\xi, \eta, \phi) = \frac{1}{\pi} R(\xi, \eta, \phi) F_0 \xi. \quad (4)$$

By definition, the flux of light F reflected by a medium is related to the intensity I by the following equation,

$$F = 2\pi \int_0^1 I(\xi, \eta) \eta d\eta, \quad (5)$$

where $I(\xi, \eta)$ is the azimuthally averaged value of $I(\xi, \eta, \phi)$,

$$I(\xi, \eta) = \frac{1}{2\pi} \int_0^{2\pi} I(\xi, \eta, \phi) d\phi. \quad (6)$$

Using Eqs. (4)–(6), and assuming that $R = \text{const}$, we obtain:

$$F = R F_0 \xi. \quad (7)$$

Now the physical meaning of the function R can be established. Namely, Eq. (7) gives a standard expression for the flux reflected by a Lambertian surface with the albedo R . Therefore, the constant value of R indicates that a light scattering layer behaves similar to a Lambertian surface.

In the idealized case of a complete reflection ($R=1$), we have from Eq. (4):

$$I^* = \frac{F_0 \xi}{\pi}. \quad (8)$$

Therefore, the value of R can be defined as the ratio of the measured top-of-atmosphere intensity I to the value of intensity I^* (see Eqs. (3) and (8)). This gives the physical meaning of this function.

The spatial distribution of the reflection function R over the hurricane Erin on September 13th, 2001 (16:21 UTC) is given in [Fig. 1](#). The data were obtained using SeaWiFS measurements. Then the eye of the hurricane was located approximately at 39° north latitude and 60° west longitude. Note that white color in [Fig. 1](#) corresponds to values of R larger than one. It follows from [Fig. 1](#) (see also [Fig. 2](#)) that the measured reflection function can exceed the value of $R=1$, which is characteristic for ideally white Lambertian plane-parallel surfaces. This is especially true at the hurricane wall (see [Fig. 3](#)). Note that numbers in [Figs. 1 and 3](#) (and similar figures, which follow) give coordinates of a given pixel in the scene. Because the size of a pixel is close to 1 km^2 , these numbers are close to distances in km. We see that the hurricane event takes a place over a very large area (approximately, $700*1400 \text{ km}^2$). Note also a circular layer of thin cirrus clouds on the left side of [Fig. 1](#) (see, e.g., the pixel with coordinates (150,900)).

The black area in [Fig. 1](#) corresponds to clear air with values of the reflection function smaller than 0.2. Note that the variability of R in clear pixels is low (see [Fig. 2](#)). The black color in [Fig. 1](#) divides the large values of reflection function in a hurricane and those in a cloud system in the left upper corner of [Fig. 1](#). Most probably, the transfer of cold arctic air takes place from north down to south, which is due to a hurricane low pressure system and its circular motion with a high speed.

We see that the atmosphere in the upper left corner of [Fig. 1](#) is almost undisturbed. This is not the case for the lower part of [Fig. 1](#), where there are a lot of scattered clouds. This indicates the direction of the hurricane (from south to the north) in this particular case. The reflection function distribution for the whole case ($850*1700=1,445,000$ pixels) is shown in [Fig. 2](#). The lowest value of the reflection function is equal to 0.17. The existence of this limit is due to contribution of molecular and background aerosol scattering. Also, the reflection from ocean can contribute to this signal. Values of the reflection function for clear pixels are smaller than approximately 0.3 with comparatively narrow distribution, having the maximum around 0.18 (see [Fig. 2](#)), which roughly corresponds to a background atmosphere. On the other hand, the hurricane itself has the reflection function in the range 0.5–1.0. R is distributed much more uniformly than for the case of a clear atmosphere (see [Fig. 2](#)), where there is a sharp peak.

The reflection function of the northern part of the hurricane wall (hot spot area) is shown in [Fig. 3](#). We see a very non-uniform distribution on a comparatively small scale,

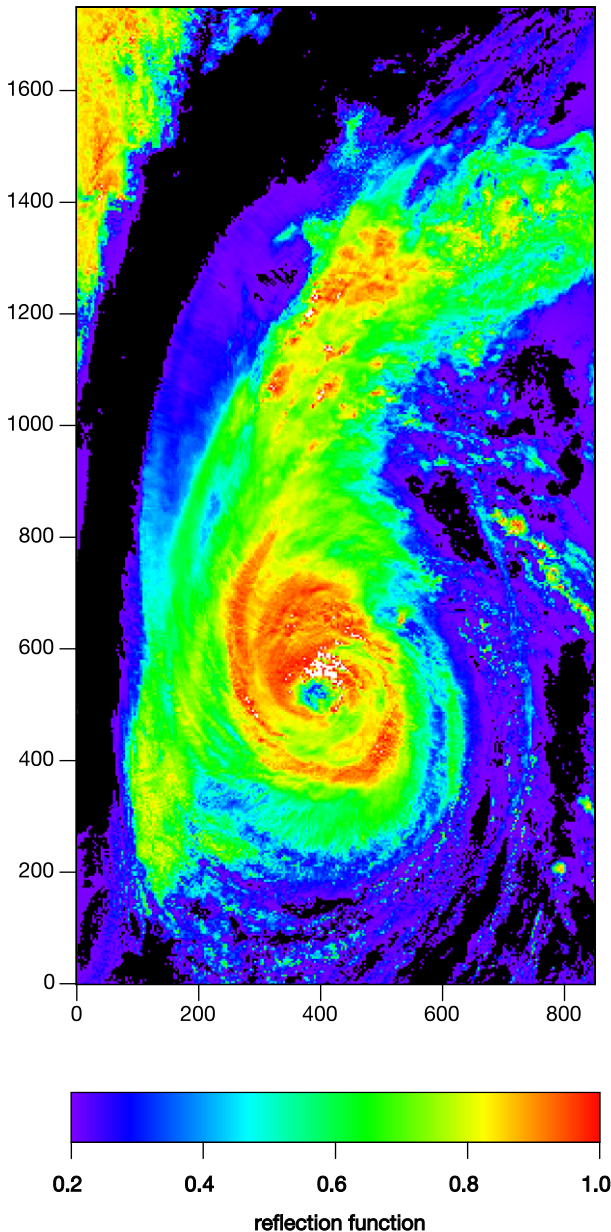


Fig. 1. The reflection function spatial distribution.

which is approximately, $30 \times 50 \text{ km}^2$. The reflection function distribution for Fig. 3 is shown in Fig. 4. It has a maximum close to $R=1.0$. The distribution is quite symmetric with larger probabilities to the left of maximum, however. It follows from Figs. 3 and 4

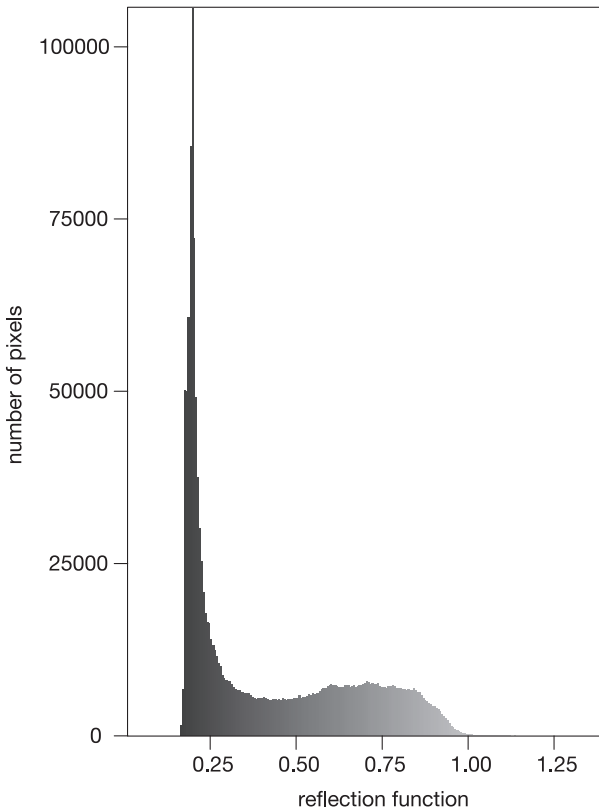


Fig. 2. The reflection function frequency distribution.

that a great portion of the hurricane's wall has values of R larger than 1. Therefore, hurricanes can reflect more light than idealized Lambertian reflectors do.

To better understand this effect, we have calculated the reflection function of a plane-parallel semi-infinite layer composed of water droplets. The results are shown in Fig. 5 for the case of the nadir observation and as the function of the solar zenith angle. We see that semi-infinite media can produce reflection functions larger than 1.0 (but smaller than 1.25, compare with Fig. 4). The same applies to the case of semi-infinite layers with nonspherical randomly oriented particles. In particular, the results of calculations for randomly oriented hexagonal columns and fractal particles are shown in Fig. 5 as well. The relative differences in R owing to the nonsphericity of particles are shown in Fig. 6. They are smaller than 10% for the nadir observation and solar angles smaller than 65° . Therefore, these differences can be neglected in practical terms (at least, for nadir looking instruments). This will be used in the paper later on.

Note that we used Cloud C1 (Deirmendjian, 1969) droplet size distribution for calculations given in Fig. 5. Exact parameters for nonspherical particles used in this study are specified in the paper by Mishchenko et al. (1999).

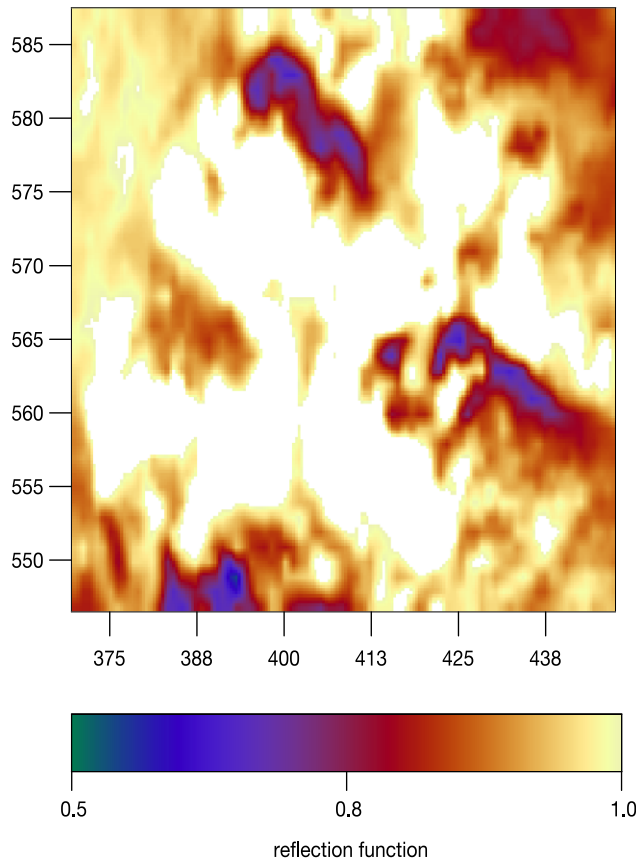


Fig. 3. The reflection function map for the hot spot area.

We also have calculated the reflection function of semi-infinite layers with spherical water droplets and ice crystals for the observation and illumination conditions, correspondent to the time of measurements (not shown here). The value of the reflection function of the semi-infinite layer was smaller than 1.0 for a whole picture given in Fig. 3 for this case. It means that the reflection function in hot spots area in Fig. 3 cannot be explained in terms of the radiative transfer theory for plane-parallel layers with water droplets and randomly oriented crystals. Layers of smaller thickness can produce only smaller values of R . This disagreement could be due to possible 3-D effects, the crystal orientation in tops of hurricanes, or both.

Modern operational cloud retrieval routines are based on the radiative transfer theory as applied to plane-parallel media (Nakajima et al., 1991). Therefore, they are not applicable for estimation of optical thickness and liquid water path in the hurricane wall. Also, operational cloud retrieval techniques are based on the study of the difference of the actual reflection function measured and the reflection function R_∞ for the case of a semi-infinite medium. Therefore, the error rapidly grows as $R \rightarrow R_\infty$.

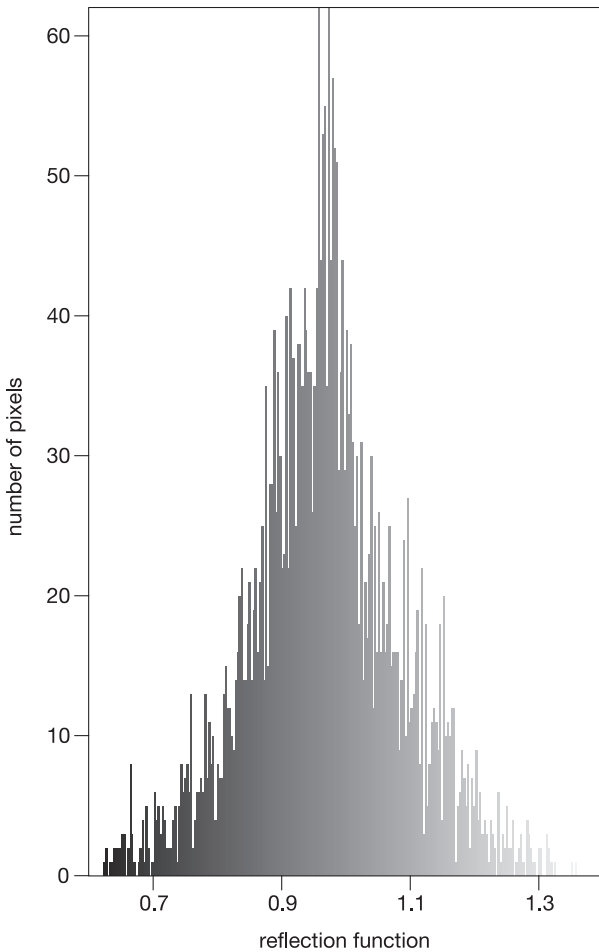


Fig. 4. The reflection function frequency distribution in the hot spot area.

Note that the hurricane eye wall area is quite small. The optical remote sensing techniques can be used for the hurricane optical thickness estimation in other parts of this case, where R does not approach R_{∞} .

To conclude, the reflection function distribution study, we consider now the area inside of the hurricane eye (see the central blue spot in Fig. 1). The enhanced picture of a hurricane eye is given in Fig. 7. It is seen that it has a random fractal shape with highly non-uniform distribution. This is due to clouds present inside the eye. The pattern differs considerably both in terms of the absolute values of the reflection function and its distribution as compared to the case of a calm ocean (blue color outside the hurricane in the upper part of Fig. 1). We conclude that hurricanes eyes could be semi-transparent and not clean of clouds.

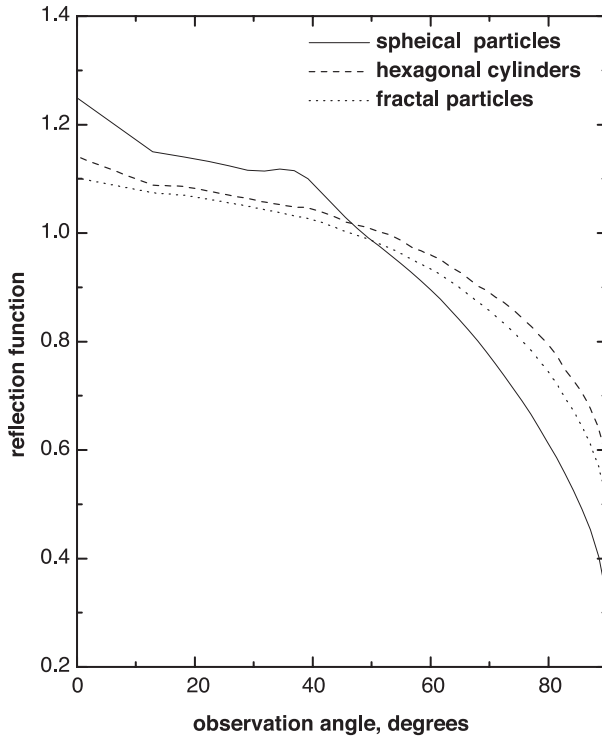


Fig. 5. The dependence of the reflection function on the shape of particles.

Therefore, the assumption of a clear undisturbed air in a hurricane eye is not always valid. We did not find such highly variable patterns as in Fig. 7 for areas which are not disturbed by the hurricane. The reflection function is almost constant in calm areas, which, in particular, explains the sharp maximum in Fig. 2 at $R=0.18$. This is a typical value of the background atmosphere over ocean for illumination and observation conditions correspondent to those in Fig. 1 (scattering angle larger than 140°). We found that the aerosol optical thickness for non-disturbed areas (upper part of Fig. 1) is close to 0.1. It is two times larger to the south of a hurricane (lower part of Fig. 1). To find this, the Bremen Aerosol Retrieval Algorithm (BAER) has been applied (von Hoyningen-Huene et al., 2003).

3. The analytical retrieval algorithm

Now consider an analytical algorithm for the retrieval of hurricane optical thickness and related parameters from the reflection function field given in Fig. 1. The cloud optical thickness is usually found using a look-up-table approach (Nakajima et al., 1991). However, due to a high optical thickness of hurricanes a simplification is possible. This is based on the asymptotic radiative transfer theory results (van de

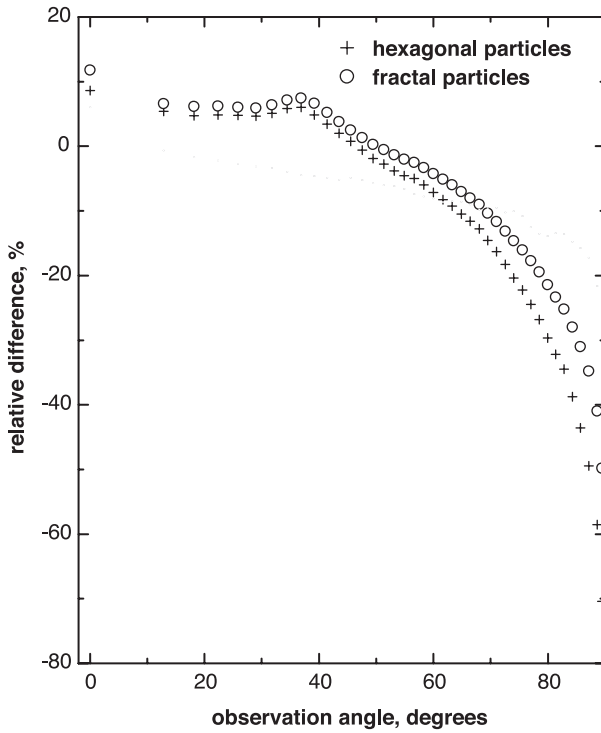


Fig. 6. The relative difference of reflection functions for hexagonal particles and fractal particles as compared to the case of spheres, obtained from data given in Fig. 5.

Hulst, 1980). Such an approach was applied to the thick cloud optical thickness τ retrievals by Rozenberg et al. (1978) and King (1987). In particular, King (1987) used the following analytical equation in his retrieval procedure,

$$R(\xi, \eta, \phi) = R_\infty(\xi, \eta, \phi) - tK(\xi)K(\eta), \quad (9)$$

where the reflection from underlying surface is neglected. Here $K(\xi)$ is the escape function (van de Hulst, 1980) and t is the global transmittance of a cloud layer, given by the following formula:

$$t = (\sigma + 0.75\tau^*)^{-1}. \quad (10)$$

Here $\tau^* = \tau(1 - g)$ is the transport (or reduced) optical thickness, g is the asymmetry parameter (King, 1987) and σ is the parameter, which is approximately equal to 1.07 for cloud phase functions (King, 1987; Kokhanovsky et al., 2003). The precise definition of functions $R_\infty(\xi, \eta, \phi)$ and $K(\xi)$ and equations for them are given by van de Hulst (1980).

The accuracy of Eq. (9) is better than 1% for clouds having the optical thickness larger than 10 (King, 1987). Therefore, it provides an excellent approximation for the hurricane

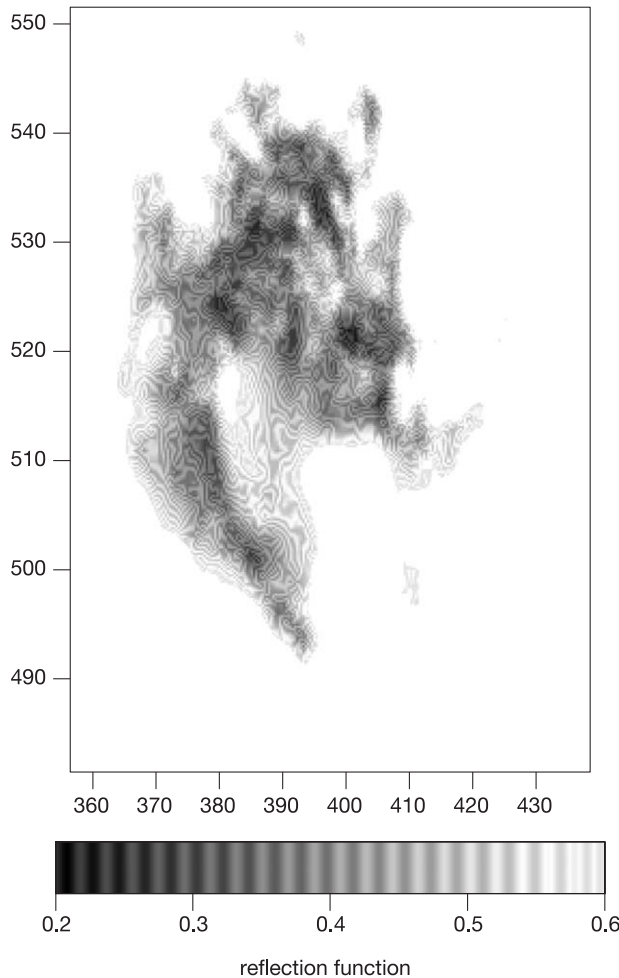


Fig. 7. The reflection function inside a hurricane eye.

scene we study (see Fig. 1). King (1987) validated the algorithm of cloud optical thickness retrieval based on Eq. (9) and found a good agreement with airborne experiments (see also Nakajima et al., 1991).

We assume here that clouds are composed of water droplets, characterized by the Deirmendjian's Cloud C1 droplet size distribution (Deirmendjian, 1969). As the modified asymptotic theory is accurate only at $\tau \geq 10$, larger retrieval errors can result for smaller cloud optical thicknesses. However, thin clouds often consist of ice crystals. Also, optically thin clouds are highly inhomogeneous. Therefore, the application of the standard radiative transfer equation for a homogeneous plane-parallel layer is not justified in this case and may lead to large retrieval errors (Loeb and Coakley, 1998). Generally, radiative properties of inhomogeneous clouds are poorly understood. So this study is mostly limited

to the case of optically thick clouds. For instance, we do not consider a band of thin cirrus clouds mentioned above (see Fig. 1).

The retrieval of the hurricane optical thickness is performed at the wavelength 412 nm, where the reflection of light from the ocean can be neglected. However, owing the large size of cloud droplets as compared to the wavelength, the optical thickness in visible region of the electromagnetic spectrum almost does not depend on the wavelength. So results obtained can be extrapolated at least for the whole visible part of the electromagnetic spectrum.

The analytical equation for the transport optical thickness follows from Eqs. (9) and (10) after simple algebraic calculations. In particular, we have

$$\tau^* = \frac{4}{3}(t^{-1} - \sigma), \quad (11)$$

where (Eq. (9))

$$t = \frac{R_\infty(\xi, \eta, \phi) - R(\xi, \eta, \phi)}{K(\xi)K(\eta)}. \quad (12)$$

Note that Eq. (12) also can be used to find the cloud spherical albedo $r = 1 - t$ (even if cloud optical thickness is not known). The spherical albedo is an important parameter in climate studies. It can be expressed as a three-dimensional integral of the reflection function, involving integration on three angular variables (Kokhanovsky, 2001). Our approach allows for a simple determination of this parameter for a scene with a hurricane.

Functions $K(\xi)$ and $R_\infty(\xi, \eta, \phi)$ can be in principle pre-calculated and stored in separate files. Note that the dependence of these functions on optical characteristics of particles is comparatively low (see Figs. 5 and 6, and also results presented by Kokhanovsky et al., 2003). This is of considerable importance because it allows to avoid the consideration of the precise shape of particles in a hurricane. This shape is not known a priori.

The situation can be even further simplified, if parameterizations of these functions are used. In particular, we will use following simple parameterizations (Kokhanovsky, in press; Kokhanovsky et al., 2003):

$$K(\xi) = \frac{3}{7}(1 + 2\xi), \quad (13)$$

$$R_\infty(\xi, \eta, \phi) = \frac{a + b(\eta + \xi) + c\eta\xi + f}{4(\eta + \xi)}, \quad (14)$$

where $a = 3.944$, $b = -2.5$, $c = 10.664$, $f = p(\theta) - p^*(\xi, \eta)$, $p(\theta)$ is the phase function (van de Hulst, 1980) and $p^*(\xi, \eta)$ is the phase function averaged with respect to the azimuth (see Eq. (6)). Note that for most of the pixels the term f is small and can be neglected.

The accuracy of Eq. (13) for the function $K(\xi)$ is better than 2% at $\xi \geq 0.2$. The accuracy of the parameterization for the value of $R_\infty(\xi, \eta, \phi)$ (Eq. (14)) is better than 5% for scattering angles larger than 150° . These conditions are met in Fig. 1. Therefore, our

parameterization introduces only a small error in the retrieval procedure as compared to other possible factors (e.g., inaccuracy in the forward model).

The map of retrieved values of transport optical thickness is given in Fig. 8. We found that the value of τ^* is mostly in the range 4–10 for areas of a case with a hurricane.

We also have selected a core of a hurricane (see Fig. 1) and made the retrieval of the transport optical thickness for this special case. The map obtained is shown in Fig. 9. The statistical distribution of the transport optical thickness for this case is given in Fig. 10. The statistical distribution has three distinct maxima, correspondent to values of the transport optical thickness equal to 1, 5, and 8. They signify differences in τ^* for various parts of the hurricane (see Fig. 9). In particular, values of $\tau^*=1$ are characteristic for the hurricane eye and values of $\tau^*=5$ are due to the contribution of lower part of Fig. 9.

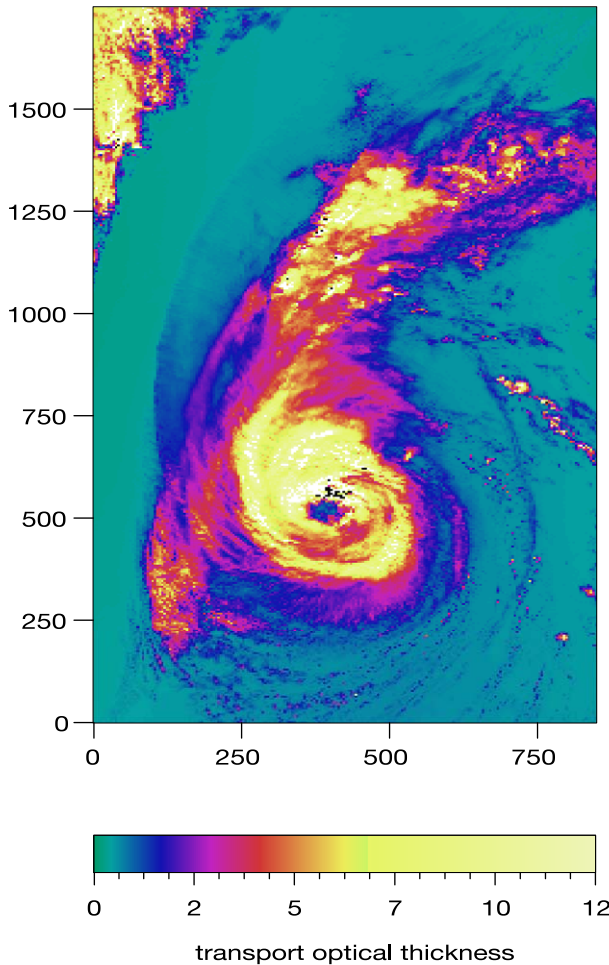


Fig. 8. The transport optical thickness map.

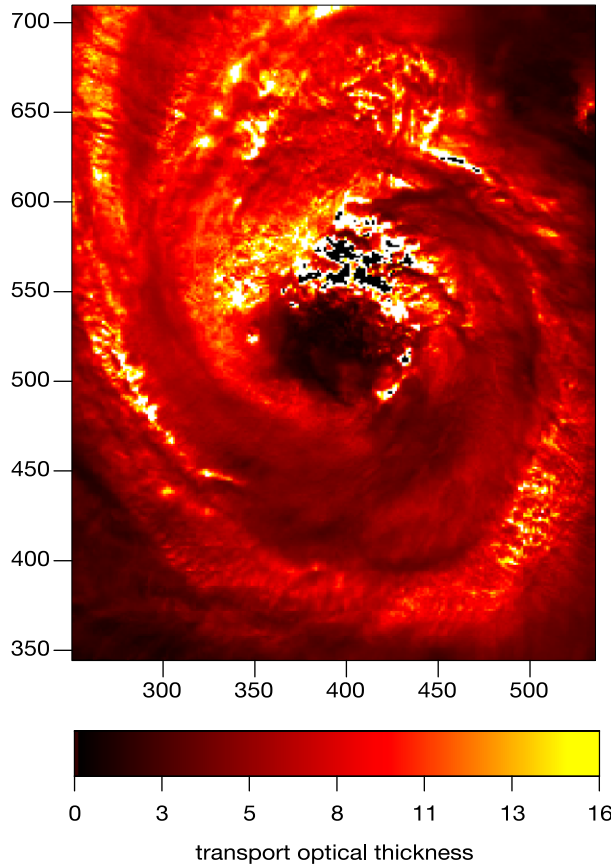


Fig. 9. The transport optical thickness of the core of the hurricane.

The values of $\tau^* = 8$ owe to the contribution from pixels that are located north of the eye.

Note also the black areas in Fig. 9 located north to the eye. They correspond to unrealistic negative values of τ^* , obtained owing to possible influence of 3-D effects as discussed above (e.g., shadowing effects).

To determine the hurricane optical thickness, the value of the asymmetry parameter g should be known. Then we have: $\tau = \tau^* / (1 - g)$. The value of g is around 0.85 for water clouds and it is close to 0.75 for ice clouds (Kokhanovsky, 2001). The retrieved cloud optical thickness distribution, assuming the value of $g = 0.85$, coincides with that given in Figs. 7–10 (but scaled using the factor $B = 1 / (1 - g)$). Note that we have at $g = 0.85$: $B = 20/3 \approx 6.7$. Therefore, the spatial distribution of τ for the case given in Fig. 9 has maxima at values close to 7, 35, and 50. Note that results at small and large values of τ can be biased because the accuracy of our technique decreases there. However, it works well for values of optical thickness in the range 10–100, which are characteristic numbers for most of pixels with a hurricane. We also found a highly non-

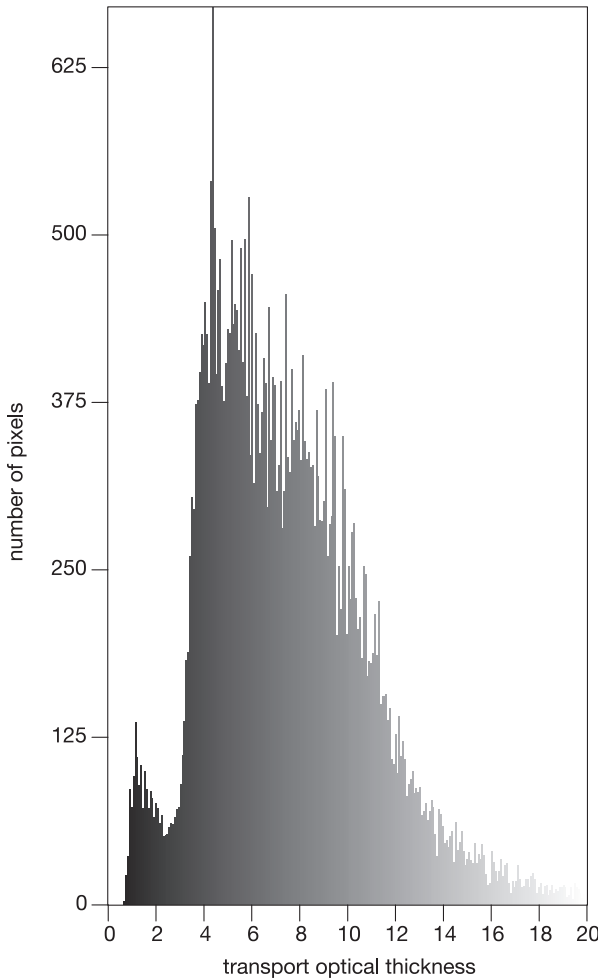


Fig. 10. The transport optical thickness distribution.

uniform distribution of cloud optical thickness in the hurricane eye similar to the distribution of R given in Fig. 7. The mode optical thickness was found to be equal seven in this case.

More studies should be done to quantify the influence of an incorrect choice of g on the hurricane optical thickness retrieval (e.g., owing to the influence of crystals, which always present in tops of hurricanes). Such crystals for sure present in the hurricane Erin.

The map of the cloud optical thickness distribution is not shown. Actually, it is the same as in Fig. 8 but scaled by the factor B . The same applies to the liquid water path W , but the scaling factor is equal to A in this case (see Eq. (1)). To estimate the value of A , we need to know the effective radius of droplets. Usually droplets have sizes

close to $10 \mu\text{m}$ (Kokhanovsky, 2001). However, particles can have larger sizes close to tops of hurricanes. Let us assume that $a_{\text{ef}}=45 \mu\text{m}$. Then we obtain that $A=30 \text{ g m}^{-2}$. Fig. 8 can be used to estimate the average liquid water path distribution in a hurricane (after multiplying the scale in Fig. 8 by the factor $C=AB \approx 200 \text{ g m}^{-2}$). In particular, the mode of the liquid water path distribution, obtained from Fig. 10, is equal approximately to 1000 g m^{-2} . However, we need to know the value of the effective radius of particles for the precise determination of W and M (see Eq. (2)). This can be obtained from near-infrared measurements (e.g., at $2.16 \mu\text{m}$), which are not available from SeaWiFS data.

To conclude, we present the hurricane spherical albedo map and frequency distribution in Figs. 11 and 12. We see that most frequent value of a hurricane albedo is around 0.86. The distribution of the spherical albedo is similar to the well-known beta distribution (Koren and Joseph, 2000), having abrupt decrease at r close to 1.0. Large values of r for a hurricane suggest that hurricanes can potentially modify planetary albedo (at least during

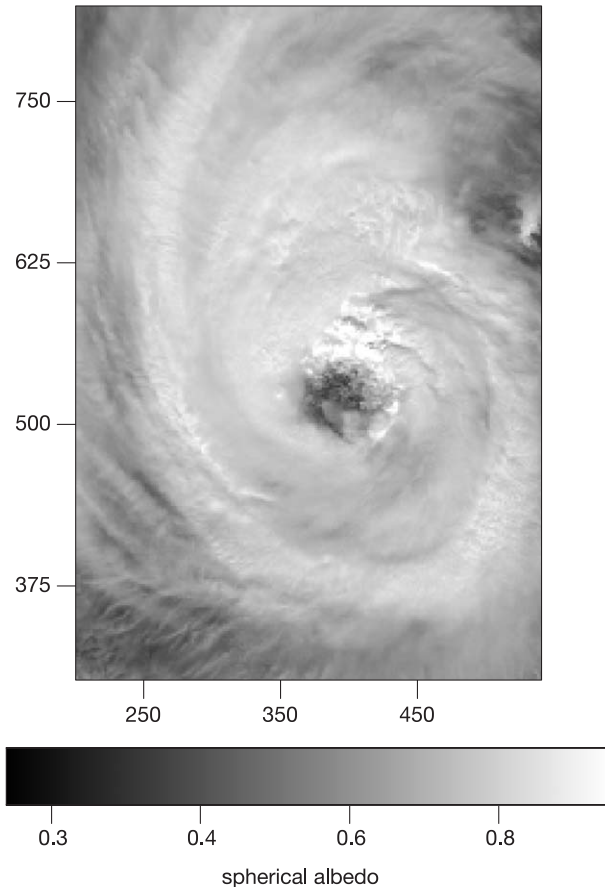


Fig. 11. The spherical albedo map.

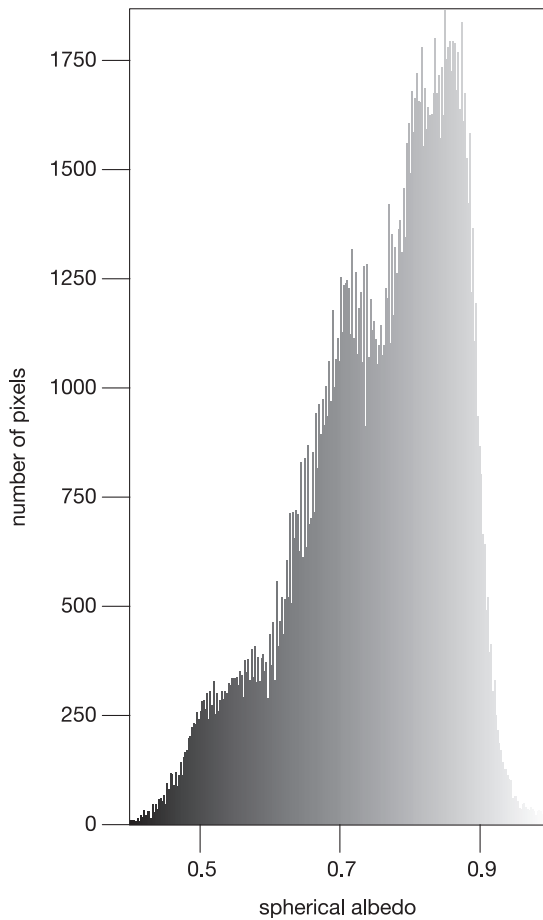


Fig. 12. The spherical albedo distribution.

the hurricane season). This can be also enhanced by foam-covered rough seas, which are produced by hurricanes.

4. Summary and conclusions

The problems and possibilities related to optical remote sensing of hurricanes have been studied. It appears that the transport optical thickness and spherical albedo of hurricanes can be retrieved using a simple analytical equation. This is of importance for processing large data sets related to hurricane cases. To obtain the optical thickness and liquid water path, the additional information is needed (g and a_{ef}). This could be in principle obtained from near-infrared measurements [e.g., using MODIS (King et al., 1992) instrument].

It is difficult to obtain the liquid water path in hurricane's walls from optical measurements owing to large values of the liquid water path there and also owing to the influence of the 3-D effects. The importance of 3-D effects in hurricane walls can also be derived from hurricane-top height retrievals, performed by [Moroney et al. \(2002\)](#). They show that the wall-top-height is at least 4 km larger than that of the rest of a hurricane. This underlines once more the importance of 3D effects (e.g., shadowing and brightness enhancement) for the wall optical remote remote sensing.

The most probable cloud optical thickness inside the hurricane eye appears to be equal to seven for hurricane Erin. This is in contrast to the fact that one would expect the eye of a hurricane to be an almost cloud-free area of relatively calm winds, due to the downwards motion of the air parcels. The explanation is that the case studied corresponds to the final stages of the hurricane life cycle shortly before dissipation. The optical thickness is larger at the eye wall and in outer band of a hurricane, where it is mostly in the range 20–100.

We also retrieved the aerosol optical thickness distribution around the hurricane, using the algorithm described by [von Hoyningen-Huene et al. \(2003\)](#). Parts of sky around hurricane appeared to be extremely clean with optical thickness 0.1 and even lower (see left top corner of [Fig. 1](#)). The atmospheric optical thickness for clear pixels to the south of a hurricane has at least two times larger values as compared to the clear pixels in the northern part of the scene. This is mostly due the influence of different air masses (clean arctic air masses from north and possibly polluted air masses from south). The passage of a hurricane itself could also increase the aerosol optical thickness due to the increase in humidity.

It should be remembered that the results derived are related to a single moment of Erin's life (September 13th, 2001, 16:21UTC) between its maximum strength on September 10th, 2001 and the dissipation on September 17th, 2001. We are going to extend this study to derive optical properties of hurricanes in statistical terms. For this, we plan to study a large number of hurricane events, using both SeaWiFS and MODIS imagery.

In conclusion, we underline that studies of hurricanes, using the combination of visible, infra-red, and microwave techniques could strongly enhance our knowledge of hurricanes.

Acknowledgements

This work has been supported in part by the University of Bremen, the German Ministry of Research and Education (BMBF) and the German Space Agency(DLR). Authors are indebted to the Ocean Color Data Support Team of the Goddard Earth Sciences Distributed Active Archive Center (Greenbelt, USA) for giving us a permission to use their data. Without this support, this work will not be possible. The authors also are indebted to M. Mishchenko for the use of the radiative transfer code to calculate the reflection function of a semi-infinite cloud with particles of various shapes.

References

Deirmendjian, D., 1969. Electromagnetic Scattering on Spherical Polydispersions. Elsevier, Amsterdam.

Fisher, J., et al., 1991. Detection of cloud-top height from backscattered radiances within the oxygen A band: Part 2. Measurements. *J. Appl. Meteorol.* 30, 1260–1267.

Goloub, P., et al., 2000. Cloud thermodynamical phase classification from the POLDER spaceborne instrument. *J. Geophys. Res.* D105, 14747–14759.

Heymsfield, G.T., et al., 2001. Doppler radar investigations of the eyewall of Hurricane Bonnie during the convection and moisture experiment-3. *J. Appl. Meteorol.* 40, 1310–1330.

King, M.D., et al., 1987. Determination of the scaled optical thickness of clouds from reflected solar radiation measurements. *J. Atmos. Sci.* 44, 1734–1751.

King, M.D., et al., 1992. Remote sensing of cloud, aerosol, and water vapour properties from the moderate resolution imaging spectrometer (MODIS). *IEEE Trans. Geosci. Electron.* 30, 2–27.

Knap, W.H., Stammes, P., Koelemeijer, R.B.A., 2002. Cloud thermodynamic-phase determination from near-infrared spectra of reflected sunlight. *J. Atmos. Sci.* 59, 83–96.

Koelemeijer, R.B.A., et al., 2001. A fast method for retrieval of cloud parameters using oxygen A band measurements from the Global Ozone Monitoring Experiment. *J. Geophys. Res.* 106 (4), 3475–3490.

Kokhanovsky, A.A., 2001. Light Scattering Media Optics: Problems and Solutions. Springer-Praxis, Chichester.

Kokhanovsky, A.A., 2003. Reflection of light from nonabsorbing semi-infinite cloudy media: a simple approximation. *J. Quant. Spectrosc. Radiat. Transfer* (in press).

Kokhanovsky, A.A., et al., 2003. A semi-analytical cloud retrieval algorithm using backscattered radiation in 0.4–2.4 spectral region. *J. Geophys. Res.*, D 108 (10.1029/2001JD001543).

Koren, I., Joseph, J.H., 2000. The histogram of the brightness distribution of clouds in high-resolution remotely sensed images. *J. Geophys. Res.*, 105, 29, 369–29, 377.

Loeb, N.G., Coakley Jr., J.A., 1998. Inference of marine stratus cloud optical depths from satellite measurements: does 1D theory apply? *J. Atmos. Sci.* 11, 215–233.

Mishchenko, M.I., et al., 1999. Bidirectional reflectance of flat, optically thick particulate layers: an efficient radiative transfer solution and applications to snow and soil surfaces. *J. Quant. Spectrosc. Radiat. Transfer* 63, 409–432.

Moroney, C., et al., 2002. Operational retrieval of cloud-top heights using MISR data. *IEEE Trans. Geosci. Remote Sens.* 40, 1532–1540.

Nakajima, T., et al., 1991. Determination of the optical thickness and effective particle radius of clouds from reflected solar radiation measurements: Part II. Marine stratocumulus observations. *J. Atmos. Sci.* 48, 728–749.

Neckel, H., Labs, D., 1989. The solar radiation between 3300 and 12500 Å. *Sol. Phys.* 90, 205–258.

Rozenberg, G.V., et al., 1978. The determination of optical characteristics of clouds from measurements of the reflected solar light using data from the Sputnik “KOSMOS-320”. *Izv.-Acad. Sci., USSR Atmos. Ocean. Phys., Engl. Transl.* 10, 14–24.

Simpson, R. (Ed.), 2002. Hurricane! Coping with disaster. American Geophysical Union, Washington.

van de Hulst, H.C., 1980. Multiple Light Scattering. Academic Press, New York.

von Hoyningen-Huene, W., et al., 2003. Retrieval of aerosol optical thickness over land surfaces from top-of-atmosphere radiance. *J. Geophys. Res.* D9 (108), 4260 (doi: 10.1029/2001JD002018).

Yamamoto, G., Wark, D.Q., 1961. Discussion of the letter by R.A. Hanel, “Determination of cloud altitude from a satellite”. *J. Geophys. Res.*, 3596.